New Features of Cervical Precancerous Cell Based on FE-SEM/EDX Line Scanning for Classification Systems

Yessi Jusman[1], Widdya Rahmalina[1], Sri Kartini[2], May Valzon[3] and Siti Nurul Aqmariah Mohd Kanafiah[4]
[1]*Department of Informatics Engineering, Faculty of Engineering, Universitas Abdurrab, Pekanbaru, 28291 Riau, Indonesia*
[2]*Department of Pharmaceutical and Food Analysts, Faculty of Medicine and Health Science, Universitas Abdurrab, Pekanbaru, 28291 Riau, Indonesia*
[3]*Department of Anatomy, Faculty of Medicine and Health Science, Universitas Abdurrab, Pekanbaru, 28291 Riau, Indonesia*
[4]*School of Mechatronic Engineering, Universiti Malaysia Perlis, Pauh Putra Campus, 02600 Arau, Perlis, Malaysia*
aqmariah@unimap.edu.my

***Abstract*— The applicability and reliability of field emission scanning electron microscopy and energy dispersive X-ray (FE-SEM/EDX) to scan structure of materials at the micro-and/or the nanoscale level, characterize the material with its elemental properties have opened this research to obtain new features from EDX spectral of cervical cells to distinguish normal and abnormal cells to be fed into classification tool. For cervical cell classification, this study proposes new features of cervical cell based on FE-SEM/EDX spectrum that are suitable and can be differentiated the cervical cell to be normal and abnormal. The cervical cell samples were extracted from SurePath®. From the SurePath®, the cervical cell samples for FE-SEM were prepared using HMDS method to obtain capable FE-SEM/EDX data. The applicability of FE-SEM/EDX data based on line scanning technique was tested by using discriminant analysis (DA) as classification tools. The result showed that the proposed features from FE-SEM/EDX techniques were applicable for cervical spectra classification in the cervical precancerous diagnostic system.**

***Index Terms*— Cervical Precancerous Cell; Classification; Data Acquisition; EDX Line Scanning; Features; FESEM.**

I. INTRODUCTION

Cervical cancer is the third most commonly diagnosed cancer and the fourth leading cause of cancer death in females worldwide, accounting for 9% (529,800) of the total new cancer cases and 8% (275,100) of the total cancer deaths among females in 2008 [1]. The cervical cells with lesion develop to be cancer over a period of two to three decades. A part of lesions during adolescence usually grew to be low grade and another part will spontaneously regress back to be normal. A small part continued to develop into true cancer precursors [2]. It was providing sufficient time for the screening of the lesion and obtain true treatment. The incident and mortality can be reduced through early detection related to this disease.

Recently, the computer-aided screening system helped the cytotechnologists and pathologists to have more confidence [3-4]. Due to the recent advancement of imaging technology, much progress has been developed in computer-aided screening system based on Pap smear [5], Thin Prep [6], colposcopy [7], cervigram [8], fluorescent in situ hybridization [9], and cervical cell FTIR [10].

Based on our knowledge in [11], the computer-aided screening system for cervical cells based on cytology samples appears as a chosen technique with better results. As stated liquid-based cytology (LBC) method, using SurePath™ and ThinPrep® Pap test, has emerged to improve the quality of smears for Cytopathologic evaluation [12-13].

By using these LBC techniques, many data acquisition approaches could be employed with the cervical cell samples to obtain cervical cell images for features extraction purposes. Field emission scanning electron microscopy (FE-SEM) is electron microscopy with a high-resolution image. The high-resolution images of FE-SEM have been promoted as better data acquisition in science and engineering fields. By using FE-SEM, cervical cell features could be extracted based on morphology and elemental compositions features as presented on [14]. FE-SEM has been successfully developed to meet the demands for recent applications requiring very high magnification (>100,000×) and a high-precision stage relative to those of traditional SEM [15], [16-18]. Therefore, FE-SEM is a very useful tool for high-resolution surface imaging in the field of nanoscale science [19]. Energy dispersive X-ray (EDX) spectroscopy has been extensively used as a chemical microanalysis technique in conjunction with advanced SEM to provide high-resolution imaging, semi-quantitative elemental analysis, and qualitative X-ray elemental maps for investigating the architecture and compositional details of different samples [20-21]. The term FE-SEM/EDX refers to the manner in which the data is collected and converted from an interference pattern to a spectrum. Perhaps, it is the most powerful tool for identifying types of elemental distribution where the wavelength of light absorbed is characteristic of the elemental producing a fluorescence absorption spectrum. Therefore, computer-aided screening system can be developed based on the cervical cell images and analyze the elemental composition of the cervical cells.

FE-SEM/EDX also has been widely used for organic material to characterize the elemental distribution on them [22-28]. For cervical cells research, [29-31] synthesized nanoparticles formulation of anticancer drug chemotherapy. The cervical cells were one of the used samples in these researches. Therefore, this study will focus on the FE-SEM approaches of extracting features from cervical cells for developing new screening system. The extracted features

from the cervical cells are classified using discriminant analysis which ready used in SPSS statistic software. The aim of this paper is to present the particle morphological structures and presented element distribution of the cervical cells which were carried out using FE-SEM.

II. Material and Methods

A. Materials

In this research, an overview of the methodology of this paper is presented in Figure 1.SurePath specimens were collected from Gribbles Pathology laboratory, Petaling Jaya, Selangor, Malaysia. The cervical cell samples investigated in this study were 60 normal, 50 LSIL, and 20 cancer cells samples. These samples were undergoing cervical screening for cervical precancerous cells. These samples were then sent to various laboratories in the faculty of dentistry, University of Malaya, Kuala Lumpur for sample preparation and capturing image process using FE-SEM. The sample preparation in this paper was based on Hexamethyldisilazane (HMDS) technique. The technique has been used in our previous research [32-33].

In principle, sample preparation for biological specimen requires three major steps (i.e. fixation, dehydration, and drying process) as presented in Figure 2. For the cervical cell in this study, the sample preparation techniques based on HMDS was employed as presented in Figure 2 and described in detail below. Sample preparation technique based on HMDS achieved good performance than conventional approach [34].

For preparing the cervical cell specimen based on the HMDS, first, the twice fixation process was implemented by rinsing the specimen with 5% glutaraldehyde in 0.1% PBS for 2 hours and osmium tetroxide for 1 hour as presented in Figure 2. Between the two fixation processes, the specimen was washed three times with 0.1% in PBS for 10 minutes each. Then, after the second fixation, the specimen was rinsed twice with deionized water for 10 minutes each.

For the dehydration process, ethanol dilution dehydration series were implemented as 50%, 75%, twice with 95% with 15 minutes each, and 3 times for 100% ethanol with an equilibration step of 20 minutes each. These processes were done only by 7 ethanol series.

In the drying process, the dehydrate specimens were immersed with 1-2 ml of HMDS for 10 minutes, then decant the HMDS from the specimen vials and leave the specimen vials with the specimen in the desiccator to air-dry at room temperature.

The final process was to mount the dried specimen on circular stainless steel molds, coated with 10 nm of pure gold in a vacuum sputter coater, and kept in a desiccator or under vacuum at all times before FE-SEM/EDX data were taken using Quanta FEG 250.

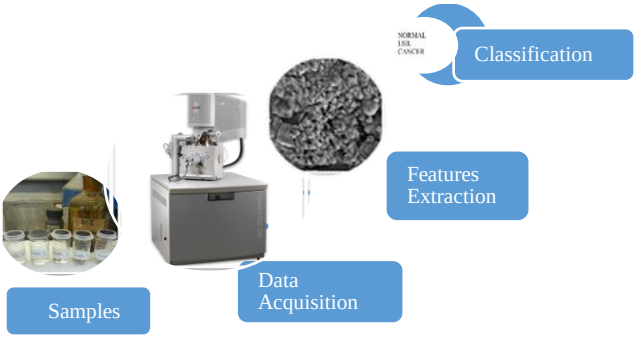

Figure 1: Overview of the methodology of this paper

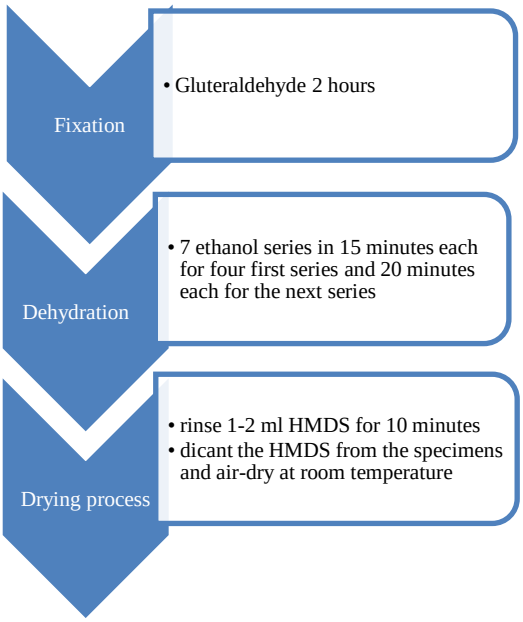

Figure 2: Sample preparation techniques based on HMDS

B. Data Acquisition

For principle operation as presented in Figure 3, FE-SEM used a focused beam of electrons to generate an image or to analyze the specimen. For operation, the gun head, the column and specimen chamber have to be evacuated. The pre-vacuum pump and turbopump evacuate the specimen chamber. The vacuum in the specimen chamber was measure by penning gauge. Column chamber valve closes and N_2 gas flows into the specimen chamber through vent valve. Schottky emitter emitted electrons. The beam of electrons passed through the multi-hole aperture. Stigmator makes sure the beam was rotationally symmetrical. Anode and linear tube were connected to form the beam booster. Beam booster provided better protection against external stray fields. Condenser lens controls the amount of demagnification. The objective lens focused the electron beam onto the specimen. Deflection system consisted of a set of scan coils to move the electron beam in a point to point scan process.

In this study, FE-SEM with brand Quanta Field Emission Gun (FEG) 250 SEM system provided flexibility and versatility to handle the challenges of today's wide-ranging research needs. In both sample preparation techniques, capturing FE-SEM imaging was implemented in the same working distance (10 mm) to produce optimal imaging condition and this distance is useful for average voltage range (5 to 20 kV). Since the overarching goal of the study was to investigate the biological samples as well as cervical cell

samples to achieve high-resolution images at high magnifications, the FE-SEM was operated at low voltage (10 to 20 kV for cervical cell samples). Both In-Lens (I-L) and Everhart-Thornley (E-T) detectors were used to image the samples.

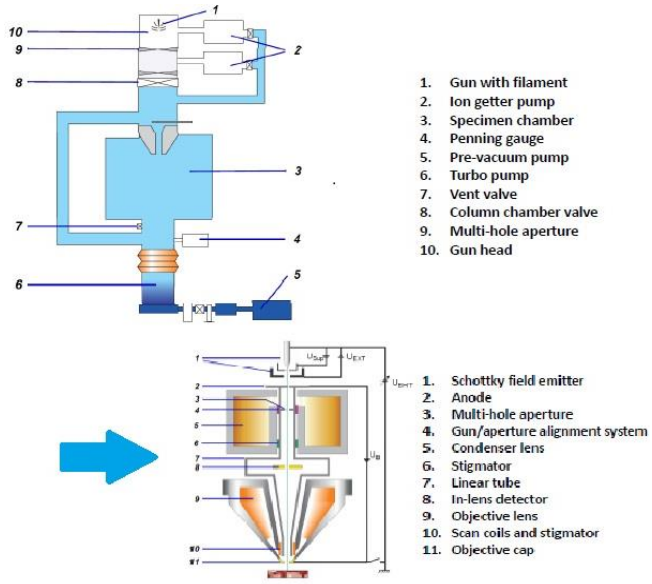

Figure 3: Principle of FE-SEM operations

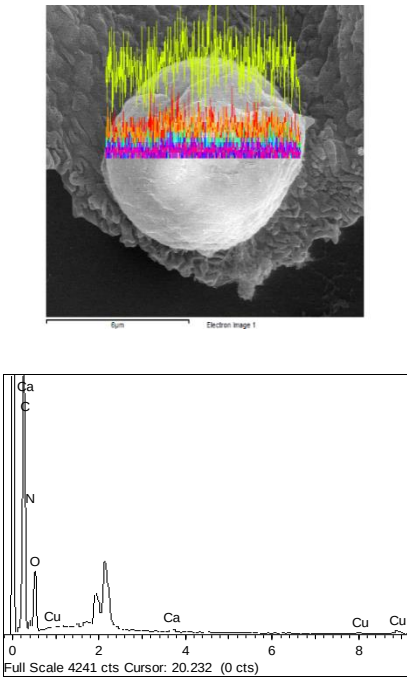

Figure 4: Cervical cell images and its EDX line scanning

The data acquisition is operated by capturing single cells and employ the EDX line scanning technique as long as the cells presented in Figure 4. The elemental distribution of the cells is produced as output for the data acquisition. For this study, the outputs of the data acquisition are 130 cell images and its EDX line scanning results as distributed as normal, LSIL, and cancer.

C. Features Extraction

In this section, the features were extracted for classification purpose. FE-SEM/EDX can produce four type of data output (i.e. FE-SEM image, EDX point spectrum, EDX line scanning spectrum, and EDX mapping area image and/or spectrum). EDX can generate images known as digital mapping, which are compositional maps of the sample. The EDX maps were recorded with a silicon drift detector and may indicate the location of each element analyzed. The brightness of the maps is related to the intensity of the pixels of the elements in the sample. EDX can identify element concentrations of <0.1 % [28]. In this work, the features were based on the EDX line scanning spectrum and mapping image and/or spectrum. The main features for classification purpose were extracted by using EDX line scanning spectrum as presented in Figure 4. For further confirmation, by mapping image, the morphological characterization was again carried out via EDX area mapping result.

In the EDX line scanning and mapping, the elemental distributions are obtained. As mention in references, the cells should contain nitrogen, oxygen, carbon, natrium, calcium, magnesium, and etc. The calcium hydroxyapatite-rich area exhibited higher amounts of Carbon (C), Oxygen (O), Phosphate (P), and Calcium (Ca) elements as well as trace amounts of Nitrogen (N), Natrium (Na), Magnesium (Mg), and Aluminium (Al), whereas the major concentration of C, minor concentrations of N and O, and trace amounts of P and Ca were observed in the cholesterol-rich area [28]. As stated in previous research, the different class of cervical cells has different chemical compound [35], [36], [37]. Therefore, in this study the elemental distribution was believed that could be found as main features to be fed into classification tools.

D. Classification

In the classification step, the discriminant analysis technique was employed to check the accuracy of normal and abnormal cell classification. Many extracted features were fed as input into the DA classification technique. The DA technique was used for features selection and classification respectively.

The current study implemented the DA using Statistical Package for the Social Sciences (SPSS) software version 14. The stepwise method was chosen for determining the optimum features (i.e. eliminate unwanted features).The optimum features were selected based on null hypothesis and p-value. The null hypothesis was rejected when the *p*-value was more than $\alpha = 0.05$ (95% confidence level).

III. RESULTS

This section involves results of data acquisition of spectrum and image from cervical cells samples, features extraction and classification. In the acquisition step, the image can be produced by FE-SEM technique and the spectrum and/or image can be resulted by EDX technique. In this study, the FE-SEM images were used as a reference for the cervical cells. Then, EDX mapping images were used to know the element contents in the cell area as presented in Figure 5. While, the EDX line scanning spectra were used to know the element contents in the line scanning in the cells as presented in Figure 4. In the features extraction step, new features from the EDX line scanning spectrum of the cervical cells were extracted as main features for differentiating the cervical cells in big amount. Therefore, in the classification step, the spectrum was used as input data for the classification system.

As stated in the previous section, the C, O, and N spectrum

were mainly due to the presence of cholesterol and protein concentrations. The P and Ca spectrum belonged to the calcium hydroxyapatite deposit. The cervical cell in this study contains C, N, O, Na, Mg, Ca, Copper (Cu), Al, Silicon (Si), Yttrium (Y), Zinc (Zn), Chlorine (Cl), Iron (Fe). The features were namely as X_1, X_2, X_3, X_4, X_5, X_6, X_7, X_8, X_9, X_{10}, X_{11}, X_{12}, and X_{13}, respectively as tabulated in Table 1.

Table 1
Featured Results from Line Scanning EDX

Features Based on Elemental Distribution	Abbreviation
Carbon (C)	X_1
Nitrogen (N)	X_2
Oxygen (O)	X_3
Natrium (Na)	X_4
Magnesium (Mg)	X_5
Calcium (Ca)	X_6
Copper (Cu)	X_7
Aluminum (Al)	X_8
Silicon (Si)	X_9
Yittrium (Y)	X_{10}
Zinc (Zn)	X_{11}
Chlorine (Cl)	X_{12}
Iron (Fe)	X_{13}

Based on the EDX line scanning technique, the probable features are presented in Table 1. Each cell has the elements but in the variety of content. As presented in [36], the normal, LSIL, HSIL, and cancer were believed having a difference in the element content. Here, in this research, the significant features were extracted by using discriminant analysis technique. This technique selects the dominant contributed features as statistical analysis. The significant features results are presented in detail in Table 2.

Table 2
Significant Features Results after Univariate and Multivariate Analysis

Step	Number of Variables	*Exact F*			
		Statistic	***df1***	***df2***	***P*-value**
1	X_1	220.879	2	127.000	**.000**
2	X_3	82.342	4	252.000	**.000**
3	X_4	71.489	6	250.000	**.000**
4	X_5	69.114	8	248.000	**.000**
5	X_6	63.730	10	246.000	**.000**
6	X_8	55.193	12	244.000	**.000**
7	X_9	49.422	14	242.000	**.000**
8	X_{10}	44.744	16	240.000	**.000**
9	X_{11}	45.207	18	238.000	**.000**
10	X_{13}	42.506	20	236.000	**.000**

**F*= variation between sample means per variation within the samples, *df*= degrees of freedom

Wilks' Lambda method with univariate and multivariate tests was applied to the analysis results. This type of analysis was needed in order to identify clusters of analysis methods. Features X_2, X_4 and X_5 have low impact on identifying process with *p*-value distribution more than 5% (95% confidence level) using univariate test. The other features showed the high impact on identifying process with p-value distribution less than 5%. Hence, the null hypothesis is rejected for the other 10 features.

Then, the 13 features have been processed using multivariate test. From the 13 features, only 10 optimum features have been chosen using the multivariate test as suitable features for cervical cell recognition. The 10 dominant features have *p*-value distribution less than 0.05. The 10 optimum features are X_1, X_3, X_4, X_5, X_6, X_8, X_9, X_{10}, X_{11}, and X_{13}. The null hypothesis of the ten features is rejected. Thus, the multivariate analysis shows that there are significant differences among three classes of cervical cells for each feature.

Based on the discriminant analysis, it is found that only 10 dominant features have the ability to classify the cervical cells into 3 groups (classes) properly. For the classification results, the discriminant analysis classification technique using 3 classes produced a good performance. Then, the classification produced better accuracy results if the data classified as 2 classes (i.e. normal and abnormal). The 50 LSIL and 20 cancer are classified as abnormal. Thus, the data is 60 normal and 70 abnormal. The overall data are 130; each data has 10 optimum features. The classification accuracy is 100% for normal (60 normal data correctly classified out of 60 overall), 84% for LSIL (42 out of 50), and 100 % for cancer (20 out of 20).

IV. DISCUSSIONS

FE-SEM was used currently for qualitative and quantitative analysis in science and engineering especially for determining the chemical structures of many inorganic and organic compounds such as drugs, ceramic, bacteria, fungi, etc. It can also be used in material identification, deformations for tissue and cells, and assessment of purity of chemical compounds. FE-SEM study on biological cells was started at the end of the 1993s and since then it has received much attention in the field of medical sciences.

The spectral features of cervical cell in our study were obtained in the energy voltage regions 0 keV to 10 keV. As stated the features were Carbon (C), Nitrogen (N), Oxygen (O), Natrium (Na), Magnesium (Mg), Calcium (Ca), Copper (Cu), Aluminum (Al), Silicon (Si), Yttrium (Y), Zinc (Zn), Chlorine (Cl), Iron (Fe). We have found that spectra of normal and abnormal (LSIL, and cancer) cervical cells were significantly different. The spectra showed significant differences for absorbance intensity of Carbon (C), Oxygen (O), Natrium (Na), Magnesium (Mg), Calcium (Ca), Aluminum (Al), Silicon (Si), Yttrium (Y), Zinc (Zn), and Iron (Fe). However, the Nitrogen (N) of the cervical cell in this experiment is constant at 0 intensity value. The Copper (Cu) and Chlorine (Cl) was found that the intensity value of the elements was not significantly different for normal, LSIL, and cancer cells. It means that the elements are contained in the same intensity value for the three classes of cells.

The accuracy of FE-SEM is dependent on the definition of 'abnormal' and 'normal' classes. If normal, LSIL, and cancer cases were considered as three different classes, the accuracy was lower than when LSIL are called 'abnormal' (i.e., grouped with LSIL and cancer). It means for the two classes (i.e. normal and abnormal classes), the difference between normal and LSIL is totally significant, and the difference between normal and cancer is totally significant. However, the difference between LSIL and cancer is not totally significant if the cervical cells classified to be three classes. 8 LSIL cells are wrongly classified as cancer. Whereas, the normal cells are totally significant difference between LSIL

and cancer, and the cancer cells are totally different to normal and LSIL.

The changes in the spectra of cells exhibiting increasing grades of abnormality (from LSIL to cancer) are subtle. Overlapping spectra are expected because the progress to cancer is a continuous process at different stages. FE-SEM could detect early chemical changes at the molecular level of cancer cells which precede morphological changes seen under light microscopy. With the improvement in FE-SEM/EDX technique such difficulty could be obviated.

V. CONCLUSIONS

This study proposed new features of the cervical cell be used for classification of cervical cells in cervical cancer diagnostic system. FE-SEM/EDX presented good results as a potential tool to differentiate cervical cells to be three classes. The quantitative results present good results for elemental distribution existing in the cells. The possible features are content of Carbon (C), Nitrogen (N), Oxygen (O), Natrium (Na), Magnesium (Mg), Calcium (Ca), Copper (Cu), Aluminum (Al), Silicon (Si), Yttrium (Y), Zinc (Zn), Chlorine (Cl), Iron (Fe) in cervical cell which are extracted by using FE-SEM/EDX system. The dominant features are extracted by using discriminant analysis technique. Hence, the significant features of the cells to differentiate the cervical cell classes are C, O, Na, Mg, Ca, Al, Si, Y, Zn, and Fe. The elemental distribution features show the high accuracy results for classification of the cervical cells. For further study, the stage involves the development of digital signal and image processing based system to extract the significant characteristics of FE-SEM/EDX data, which will be used as input data for intelligent classifier in the next stage for classification of cervical precancerous stage purpose.

ACKNOWLEDGMENT

This research is supported by Institute of Research and Community Services, Universitas Abdurrab, Indonesia, and Universiti Malaysia Perlis, Malaysia.

REFERENCES

[1] Jemal, A., et al., Global cancer statistics. CA: a cancer journal for clinicians, 2011. 61(2): p. 69-90.
[2] Cronjé, H.S., Screening for cervical cancer in the developing world. Best Pract Res Cl Ob 2005. 19(4): p. 517-529.
[3] Lozano, R., Comparison of computer-assisted and manual screening of cervical cytology. Gynecol Oncol 2007. 104(1): p. 134-138.
[4] Rekhi, B., et al., Spectrum of neuroendocrine carcinomas of the uterine cervix, including histopathologic features, terminology, immunohistochemical profile, and clinical outcomes in a series of 50 cases from a single institution in India. Annals of Diagnostic Pathology, 2013. 17(1): p. 1-9.
[5] Mat-Isa, N.A., M.Y. Mashor, and N.H. Othman, An automated cervical pre-cancerous diagnostic system. Artif Intell Med, 2008. 42(1): p. 1-11.
[6] Harandi, N.M., et al., An automated method for segmentation of epithelial cervical cells in images of Thin Prep. J Med Syst 2010. 34(6): p. 1043-1058.
[7] van Raad, V., X. Zhiyun, and L. Holger, Lesion Margin Analysis for Automated Classification of Cervical Cancer Lesions, 2006, STI Medical Systems: Honolulu.
[8] Alush, A., H. Greenspan, and J. Goldberger, Automated and interactive lesion detection and segmentation in uterine cervix images. IEEE T Med Imaging 2010. 29(2): p. 488-501.
[9] Kajtár, B., et al., Automated fluorescent in situ hybridization (FISH) analysis of t (9;22)(q34;q11) in interphase nuclei. Cytometry Part A, 2006. 69(6): p. 506-514.
[10] Jusman, Y., et al., Intelligent classification of cervical pre-cancerous cells based on the FTIR spectra. Ain Shams Eng J, 2012. 3(1): p. 61-70.
[11] Jusman, Y., S.C. Ng, and N.A. Abu Osman, Intelligent Screening Systems for Cervical Cancer. Scientific World Journal, 2014. 2014: p. 1-15.
[12] Fremont-Smith, M., et al., Comparison of the Surepath™ liquid-based Papanicolaou smear with the conventional Papanicolaou smear in a multisite direct-to-vial study. Cancer cytopathology, 2004. 102(5): p. 269-279.
[13] Sykes, P., et al., A randomised comparison of SurePath liquid-based cytology and conventional smear cytology in a colposcopy clinic setting. BJOG: An International Journal of Obstetrics & Gynaecology, 2008. 115(11): p. 1375-1381.
[14] Taylor, C.P., et al., Oxygen/glucose deprivation in hippocampal slices: altered intraneuronal elemental composition predicts structural and functional damage. J neurosci, 1999. 19(2): p. 619-629.
[15] Roach, P., et al., Modern biomaterials: a review—bulk properties and implications of surface modifications. Journal of Materials Science: Materials in Medicine, 2007. 18(7): p. 1263-1277.
[16] Ali, S.H.R., Advanced nanomeasuring techniques for surface characterization. ISRN Optics, 2012. 2012.
[17] Pawley, J., The development of field-emission scanning electron microscopy for imaging biological surfaces. Scanning, 1997. 19: p. 324-336.
[18] Cazaux, J., Recent developments and new strategies in scanning electron microscopy. Journal of microscopy, 2005. 217(1): p. 16-35.
[19] Chien, Y.C., et al., Comparative study of nanoscale surface structures of calcite microcrystals using FE-SEM, AFM, and TEM. Microscopy and Microanalysis, 2006. 12(04): p. 302-310.
[20] Goldstein, J., et al., Scanning electron microscopy and x-ray microanalysis in ISBN2003.
[21] Piburn, G. and A.R. Barron, An introduction to energy dispersive X-ray spectroscopy, in Physical methods in chemistry and nano science. 2013: Connexions/Rice University, Houston. p. 90-98.
[22] Kaminskyj, S.G. and T.E. Dahms, High spatial resolution surface imaging and analysis of fungal cells using SEM and AFM. Micron, 2008. 39(4): p. 349-361.
[23] Godin, M., et al., Measuring the mass, density, and size of particles and cells using a suspended microchannel resonator. Applied Physics Letters, 2007. 91(12): p. -.
[24] Burg, T.P., et al., Weighing of biomolecules, single cells and single nanoparticles in fluid. Nature, 2007. 446(7139): p. 1066-1069.
[25] Park, K., et al., 'Living cantilever arrays' for characterization of mass of single live cells in fluids. Lab on a Chip, 2008. 8(7): p. 1034-1041.
[26] Congiu, T., et al., Scanning electron microscopy examination of endothelium morphology in human carotid plaques. Micron, 2010. 41(5): p. 532-536.
[27] Parameswaran, S. and R.S. Verma, Scanning electron microscopy preparation protocol for differentiated stem cells. Anal biochem 2011. 416(2): p. 186-190.
[28] Chang, H.H., et al., Application of scanning electron microscopy and X-ray microanalysis: FE-SEM, ESEM-EDS, and EDS mapping for studying the characteristics of topographical microstructure and elemental mapping of human cardiac calcified deposition. Analytical and bioanalytical chemistry, 2014. 406(1): p. 359-366.
[29] Ma, Y., et al., Nanoparticle formulation of poly(ε-caprolactone-co-lactide)-D-a-tocopheryl polyethylene glycol 1000 succinate random copolymer for cervical cancer treatment. Polymer, 2010. 51(25): p. 5952-5959.
[30] Wahab, R., et al., Fabrication and growth mechanism of ZnO nanostructures and their cytotoxic effect on human brain tumor U87, cervical cancer HeLa, and normal HEK cells. J BiolInorg Chem, 2011. 16(3): p. 431-442.
[31] Zeng, X., et al., Cholic acid-functionalized nanoparticles of star-shaped PLGA-vitamin E TPGS copolymer for docetaxel delivery to cervical cancer. Biomaterials, 2013. 34(25): p. 6058-6067.
[32] Jusman, Y., et al., A system for detection of cervical precancerous in field emission scanning electron microscope images using texture features. Journal of Innovative Optical Health Sciences, 2016: p. 1650045.
[33] Jusman, Y., et al., Computer-aided screening system for cervical precancerous cells based on field emission scanning electron microscopy and energy dispersive x-ray images and spectra. Optical Engineering, 2016. 55(10): p. 103110-103110.
[34] Moran, P. and B. Coats, Biological Sample Preparation for SEM Imaging of Porcine Retina. Microscopy Today, 2012. 20(02): p. 28-31.
[35] Wood, B.R., et al., Fourier transform infrared (FTIR) spectral mapping of the cervical transformation zone, and dysplastic squamous epithelium. Gynecologic Oncology, 2004. 93(1): p. 59-68.

[36] El-Tawil, S.G., et al., Comparative study between Pap smear cytology and FTIR spectroscopy: A new tool for screening for cervical cancer. Pathology, 2008. 40(6): p. 600-603.
[37] Chilakapati, M., et al., An overview on applications of optical spectroscopy in cervical cancers. Journal of Cancer Research and Therapeutics, 2008. 4(1): p. 26-36.G. O. Young, "Synthetic structure of industrial plastics (Book style with paper title and editor)," in Plastics, 2nd ed. vol. 3, J. Peters, Ed. New York: McGraw-Hill, 1964, pp. 15–64.